nature materials

SUPPLEMENTARY INFORMATION

DOI: 10.1038/NMAT3334

Giant magnetocaloric effect driven by structural transitions

Transition distribution model for simulating adiabatic temperature change (in Page 1-8):

The martensitic transition of Heusler alloys is described by the four characteristic temperatures A_s, A_f, M_s and M_f, which define the start and finish temperatures of austenite and martensite phases, respectively. A schematic magnetization vs. temperature curve $M(T)$ is shown in Figure M1 alongside the case for an ideal first-order transition, which would display a discontinuity in magnetization. The broadening of the transition is related to the existence of a distribution of transition temperatures over the sample volume.

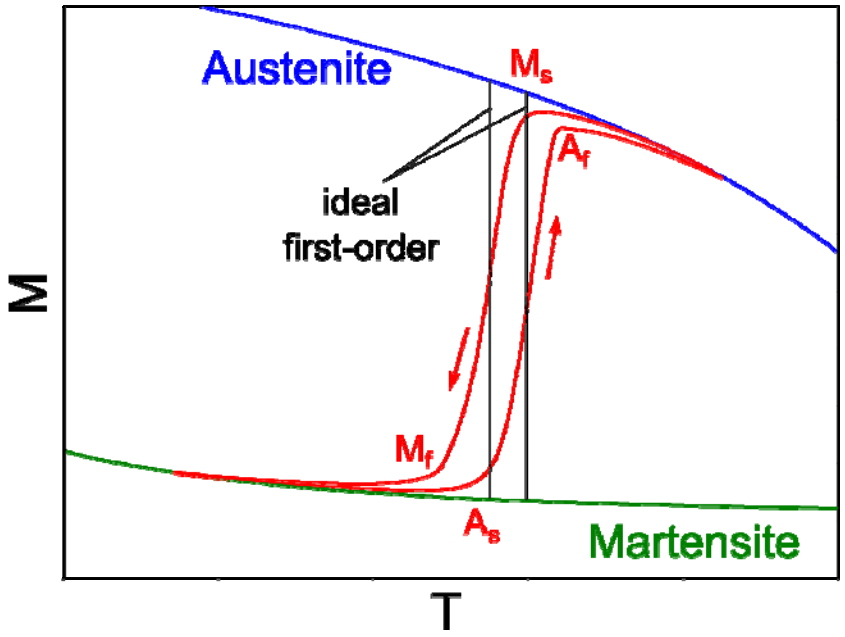

Supplementary Figure M1:
Schematic of magnetization vs. temperature curves showing the ideal and actual cases of martensite to austenite transition for Heusler alloys.

The transition distribution function $v(T)$, here referring to the statistical density of varying transition temperatures, can be estimated from $M(T)$ data. We take an alloy of $Ni_{49.8}Mn_{35}In_{15.2}$ as an example. The metamagnetic structural transition takes place due to the difference in magnetization between martensite $M_M(T)$ and austenite $M_A(T)$. To

DOI: 10.1038/NMAT3334

determine $v(T)$, it is necessary to first normalize the magnetization data in the following way

$$f(T) = \frac{M_{sample} - M_M(T)}{M_A(T) - M_M(T)} \qquad (1).$$

To keep the model simple, we consider only the heating direction in Figure M1. The normalized curve $f(T)$ is plotted in Figure M2(a) and it is to be interpreted as the volume fraction of austenite in the sample at a certain temperature. To obtain the transition distribution as shown in Figure M2(b), one needs to differentiate $f(T)$ with respect to T. We found that $v(T)$ from experimental data closely follows the Gaussian function given below in Eq. (2), where the Gaussian peak approximately coincides with T_p (transition peak temperature):

$$v(T) = \frac{1}{\sigma\sqrt{2\pi}} \cdot e^{-\frac{(T-T_p)^2}{2\sigma^2}} \qquad (2).$$

This equation is valid in the absence of a magnetic field. For the case of our Heusler alloys, the application of a magnetic field shifts T_p to lower temperatures linearly with a rate of m but keeps the distribution shape almost unchanged, as shown in the inset of Figure M2(b). We include the effect of magnetic field in Eq. (2) by adding an extra term to the exponent

$$v(T,H) = \frac{1}{\sigma\sqrt{2\pi}} \cdot e^{-\frac{(T-T_p-mH)^2}{2\sigma^2}} \qquad (3).$$

The corresponding volume fraction of austenite $f(T,H)$ at temperature T and magnetic field H is given by integrating Eq. (3) from the limits -∞ to T. The result in Eq. (4) cannot be solved analytically, so we must use a numerical method.

$$f(T,H) = \int_{-\infty}^{T} v(T',H)dT' \qquad (4).$$

Assuming that the transition from full martensite to full austenite can be completed by the application of a magnetic field under adiabatic conditions, the latent heat ΔQ is released or absorbed depending on an exothermic or endothermic transition, and results in a temperature change of the *entire* sample:

$$\Delta Q = C_p \Delta T \qquad (5),$$

where C_p is the heat capacity out of transition range under constant pressure. We found that the heat capacity in martensite and austenite phase is nearly the same. If only a small volume fraction df of austenite transforms, consequently Eq. (5) will be reduced by the phase fraction amount. Replacing $\Delta Q = T\Delta S$ in Eq. (5) (where ΔS is the isothermal entropy change) and using the phase fraction df, we find the fractional temperature change as:

$$dT = \frac{T\Delta S}{C_p} \cdot df = \tau \cdot df \qquad (6),$$

We assume the temperature is always uniform across the sample volume. The parameter τ indicates the maximum temperature change when 100% of the transformation occurs. The entropy change can be estimated using the Clausius-Clayperon equation

$$\Delta S = \frac{dH}{dT_p} \cdot \Delta M = \frac{\Delta M}{m} \qquad (7),$$

where ΔM is the difference in magnetization between martensite and austenite, and m is the change of transition temperatures by application field. Based on these considerations it is possible to simulate the adiabatic temperature change of the sample when a magnetic field is applied using the three variable parameters of field dependency m, transition width σ, and the maximum temperature change τ.

To illustrate the simulation procedure, we first consider the application of one field increment dH. The mechanism is described in Figure M3. Before the application of the field step dH, the initial phase state contains a certain amount of austenite at the temperature T_{start}. This fraction is the area under the curve (green area) up to T_{start}. If the field is increased the distribution is shifted from $v(T, H)$ to $v(T, H + dH)$. The new fraction of austenite would be shown by the red striped area if the temperature T_{start} would be kept constant (isothermal conditions).

DOI: 10.1038/NMAT3334

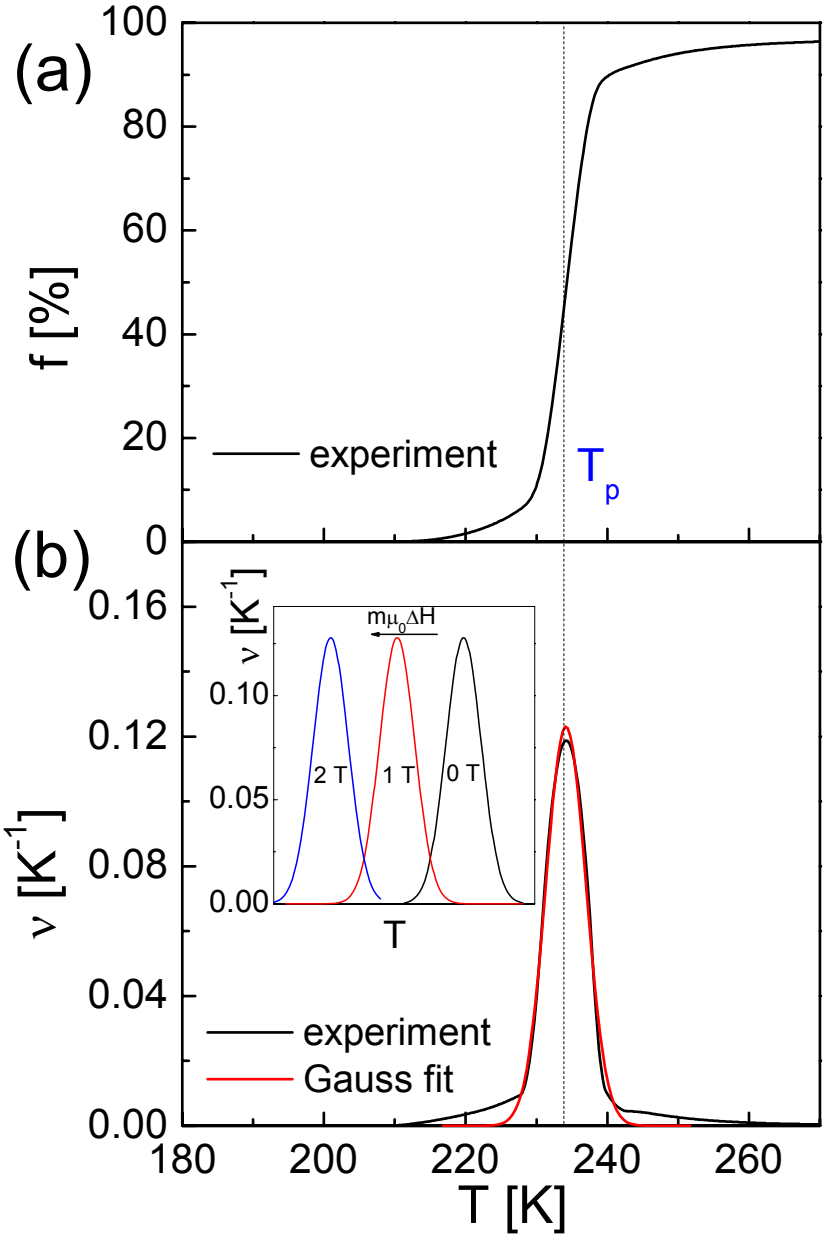

Supplementary Figure M2:
Normalized magnetization curve (a) implies the volume fraction of austenite in the $Ni_{49.8}Mn_{35}In_{15.2}$ sample. The corresponding transition distribution (b) is the first derivative of the normalized magnetization curve. It fits well with a Gaussian function. The inset shows how the distribution shifts to lower temperatures under application of a magnetic field. This behavior implies an inverse magnetocaloric effect.

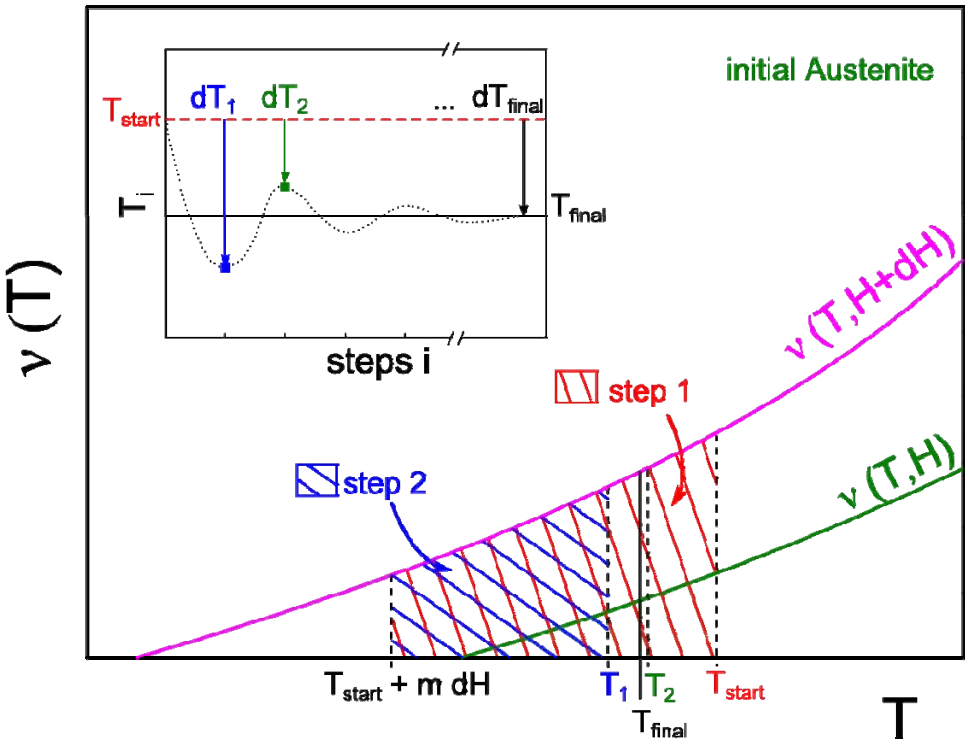

Supplementary Figure M3:
Enlarged view of the transition distribution. It describes the detail in calculating the temperature change caused by the application of one field step.

However adiabatic conditions make these calculations much more complex because the sample transforms and cools down simultaneously. We solve this by applying an iterative procedure. The fraction change after the iterative step *i* can be estimated by

$$df_i = \int_{-\infty}^{T_i} \nu(T', H + dH)dT' - \int_{-\infty}^{T_{start}} \nu(T', H)dT' \qquad (8)$$

This leads to a cooling of the sample from T_{start} to T_1 by dT_1 based on Equation (6). It means if the temperature decreases to T_1, at the same time the transformed austenite cannot be as much as calculated in the first iteration step. Therefore, the amount of transformed austenite was overestimated. Nevertheless we take this value as the starting point. The next step is to calculate the area up to T_1 (blue striped area). This area is smaller than the red striped one. The corresponding "new" temperature change dT_2 will also be smaller than dT_1. This means that the sample does not cool down so much to T_1, but should be to a bit higher temperature e.g. T_2. Now the calculated temperature T_2 is more close to the real, final temperature T_{final} after the application of a field step. To

DOI: 10.1038/NMAT3334

approach T_{final}, many repetitions of the above procedure are necessary. The inset in Figure M3 shows the typical convergence behavior of the procedure. The iteration process is needed for each small field step dH. The total adiabatic temperature change due to the field change ΔH is found by summing the contribution from dH.

We next study the influence of the controlling parameters. The field dependency m can be determined from $M(T)$ data taken in different constant magnetic fields. According to Eq. (6) and (7), if m is increased, τ will be decreased. Figure M4 shows the adiabatic temperature change behaviour for different values of m at a constant σ. It can be seen increasing m lowers the field needed to fully transform the sample. However, m also defines the maximum cooling rate that can be achieved. An optimal value of m is determined to be about -6 K/T, resulting in a full transformation with the largest temperature change in a magnetic field of 2 T. Higher m leads to a smaller τ, the resulting cooling effect will therefore decrease. Since the model also includes the conventional magnetocaloric effect of austenite, the sample temperature raises after forming a full austenite by further increasing magnetic field. This is reflected by a minimum in temperature change in Figure M4.

Next we vary the peak width σ. We take σ as being the full-width-at-half-maximum (FWHM). The relation between FWHM and σ is:

$$\mathrm{FWHM} = 2\sqrt{2\ln 2}\cdot\sigma \qquad (9).$$

We keep T_p (mid-point of the Gaussian peak), τ and m constant and vary FWHM. Both the transition distribution and the cooling behavior are plotted in Figure M5. Naturally the smaller the FWHM, the higher the peak will be because the area under the curve has to be 1. It can be seen in the cooling plot that the transition is approaching more and more the ideal first-order case when the distribution becomes sharper. But the real condition is always far from the ideal case due to the transition distribution. When the initial temperature is close to the peak temperature T_p, the sample has already contained some amount of austenite prior to the field application (especially for a broad transition as seen in the curve of FWHM = 8 K), therefore a full transition cannot take place. Secondly, the conventional magnetocaloric effect of austenite counteracts the net cooling effect.

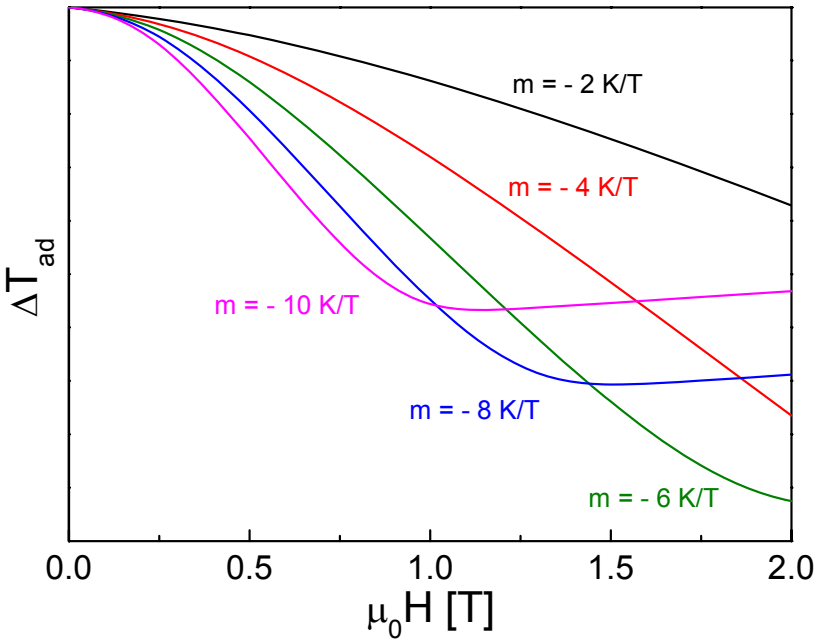

Supplementary Figure M4
A larger field dependency enables the full transformation at lower magnetic fields. A value of about -6 K/T seems to be optimal leading to the largest temperature change in 2 T. The existence of a minimum for *m* = -8 K/T and -10 K/T is due to the conventional magnetocaloric effect of austenite which is also considered in the simulation.

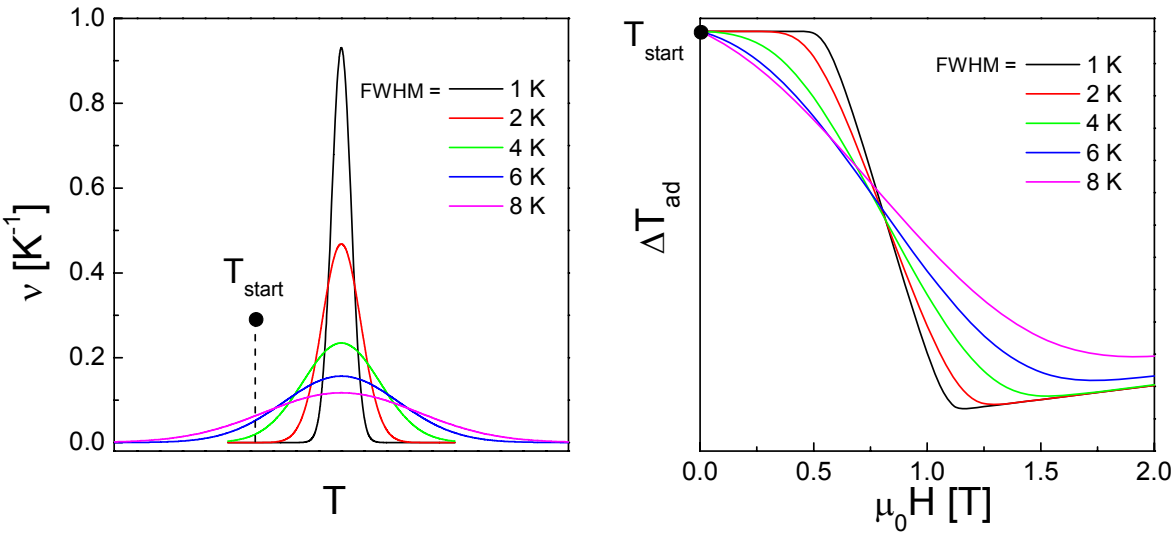

Supplementary Figure M5
Transition distribution (left) and cooling behavior (right) at different values of transition width at a constant starting temperature.

DOI: 10.1038/NMAT3334

For the development of novel magnetocaloric materials, m should be large enough to ensure the full transformation at low magnetic fields. The best case for m would be if the transition is finished exactly when the maximum magnetic field is reached because any further increase of m would lead to the decrease of the potential temperature change τ and the occurrence of conventional magnetocaloric effect of austenite. Furthermore a sharp transition is desirable to eliminate the pre-existing austenite and minimize the conventional magnetocaloric effect. In practise, however, the three controlling parameters are not independent from each other. For instance, the $Ni_{50.4}Mn_{34.8}In_{15.8}$ alloy (shown in the main body of our paper) with a too large field dependency very often has a broad transition width and a small potential cooling effect. Therefore, the optimization of these key parameters is quite necessary.

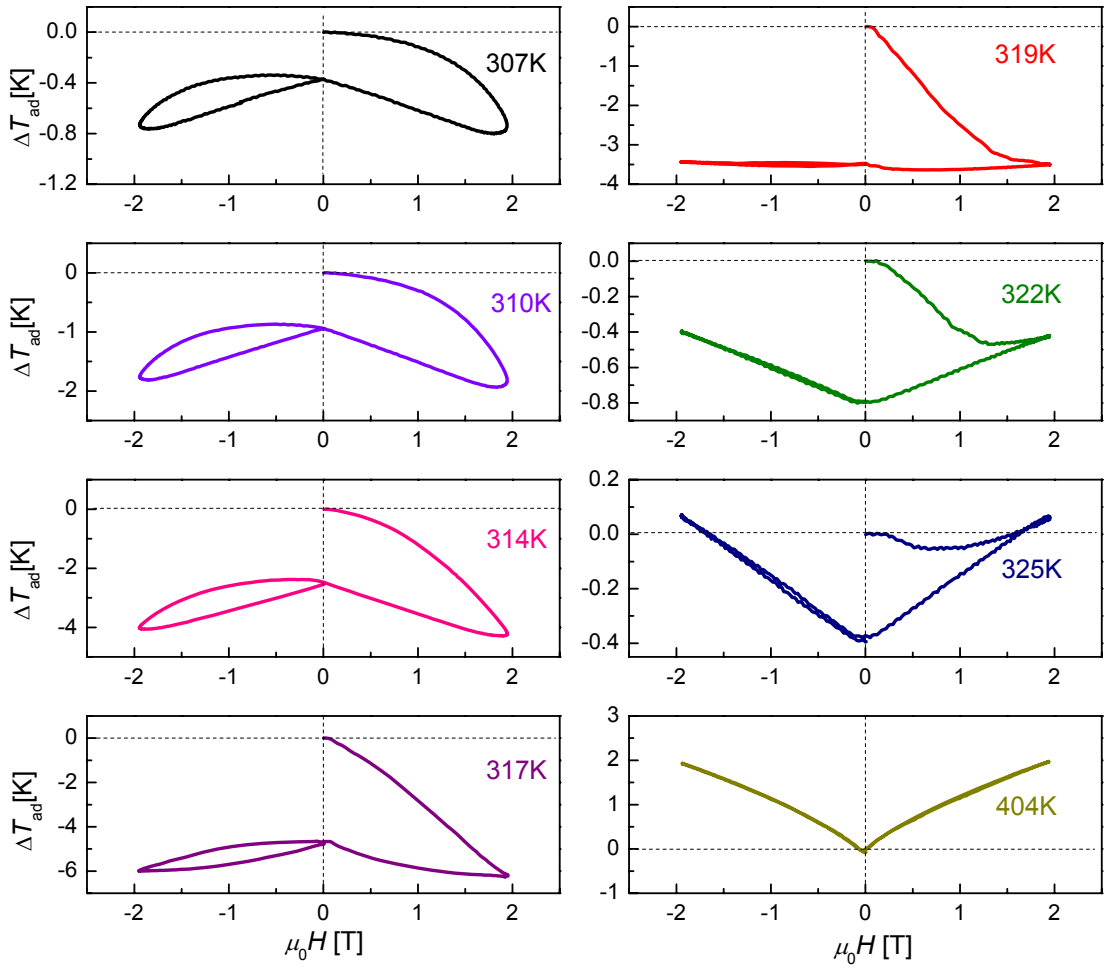

Supplementary Figure S1:
Magnetic field dependence of the adiabatic temperature change at various temperatures for $Ni_{45.2}Mn_{36.7}In_{13}Co_{5.1}$.

DOI: 10.1038/NMAT3334

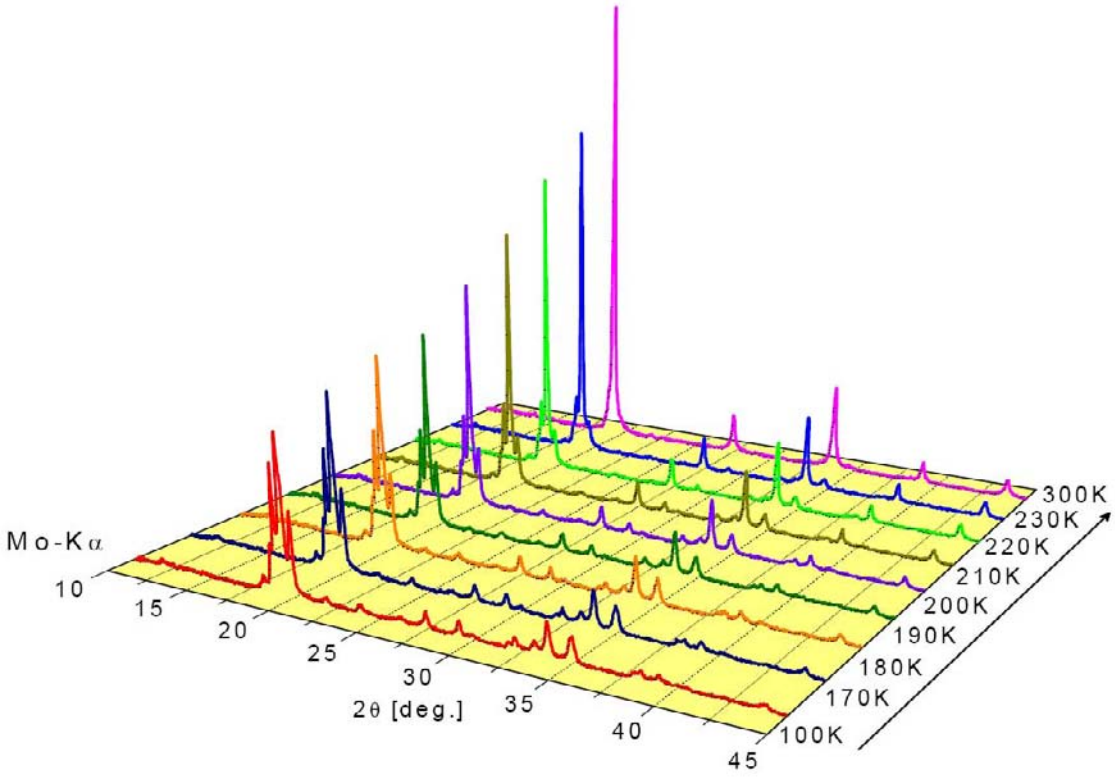

Supplementary Figure S2:
XRD patterns at various temperatures for $Ni_{50.4}Mn_{34.8}In_{15.8}$, showing the evolution of crystal structure due to martensitic transformation. The lattice parameters for martensitic and austenitic phase were calculated from patterns measured at 100 and 300 K, respectively.

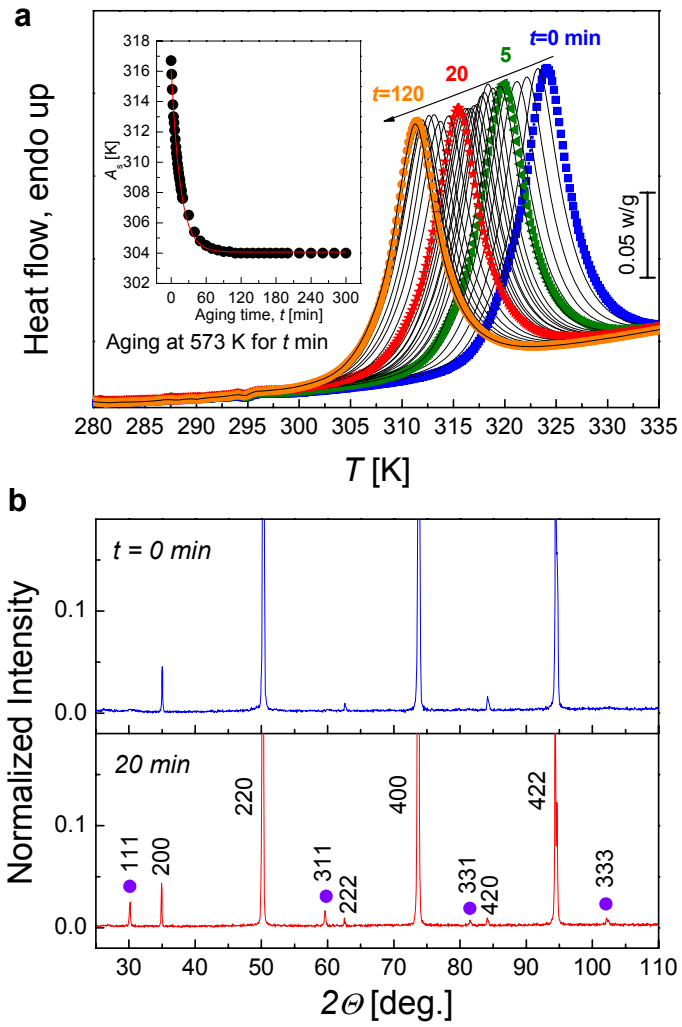

Supplementary Figure S3:
DSC curves after aging $Ni_{45.2}Mn_{36.7}In_{13}Co_{5.1}$ for different times (**a**). The inset of (**a**) shows that an accurate tuning of austenite start temperature, A_s, in a range of 317-304 K can be accomplished by aging within one hour. Room temperature XRD patterns (**b**) are taken from $Ni_{45.7}Mn_{36.3}In_{13}Co_5$ samples upon aging at 573 K. The aging induced enhancement of diffraction intensity of several $L2_1$ superlattice reflections such as (111), (311), (331) and (333) peaks are marked by circles. The relative intensity of I(111)/I(220) significantly increases from 0.005 to 0.025 by aging for 20 min.

DOI: 10.1038/NMAT3334

Description of adiabatic temperature change ΔT_{ad} measurements:

ΔT_{ad} measurements are performed in a home-built experimental setup. The magnetic field is produced by permanent magnets in a Halbach-cylinder assembly. The external magnetic field is measured by a Hall probe. The maximum field in the bore centre is 1.93 T. The magnetic field change rate is 0.5 T/s that is fast enough to neglect the heat losses from the specimen to the environment during the measurement. The temperature changes of the sample are monitored with accuracy better than ±0.01 K by a Copper-Constantan thermocouple (T-type) which was in direct contact with the sample. The measurement cell is schematically shown in Figure S5a. Two sample plates (approximate size 4 × 2 × 1 mm) with a thermocouple placed between the pieces are glued by a small amount of thermo-conductive silver-based UVH glue to improve the thermal contact. The sample holder is equipped with a resistive electric heater. During the measurements, the target temperature is approached without overheating/overcooling. The sample chamber is connected to a pump providing vacuum ~ 10^{-6} mbar and is inserted into a liquid nitrogen Dewar. After pre-amplification, the signals from thermocouple and Hall probe are collected using an analogue-to-digital converter with a sampling time of 1000 points/s. ΔT_{ad} is measured at a certain temperature as a function of the magnetic field H. Excellent adiabatic conditions are confirmed by measurements on a polycrystalline Gd sample, as shown in Figure S5b.

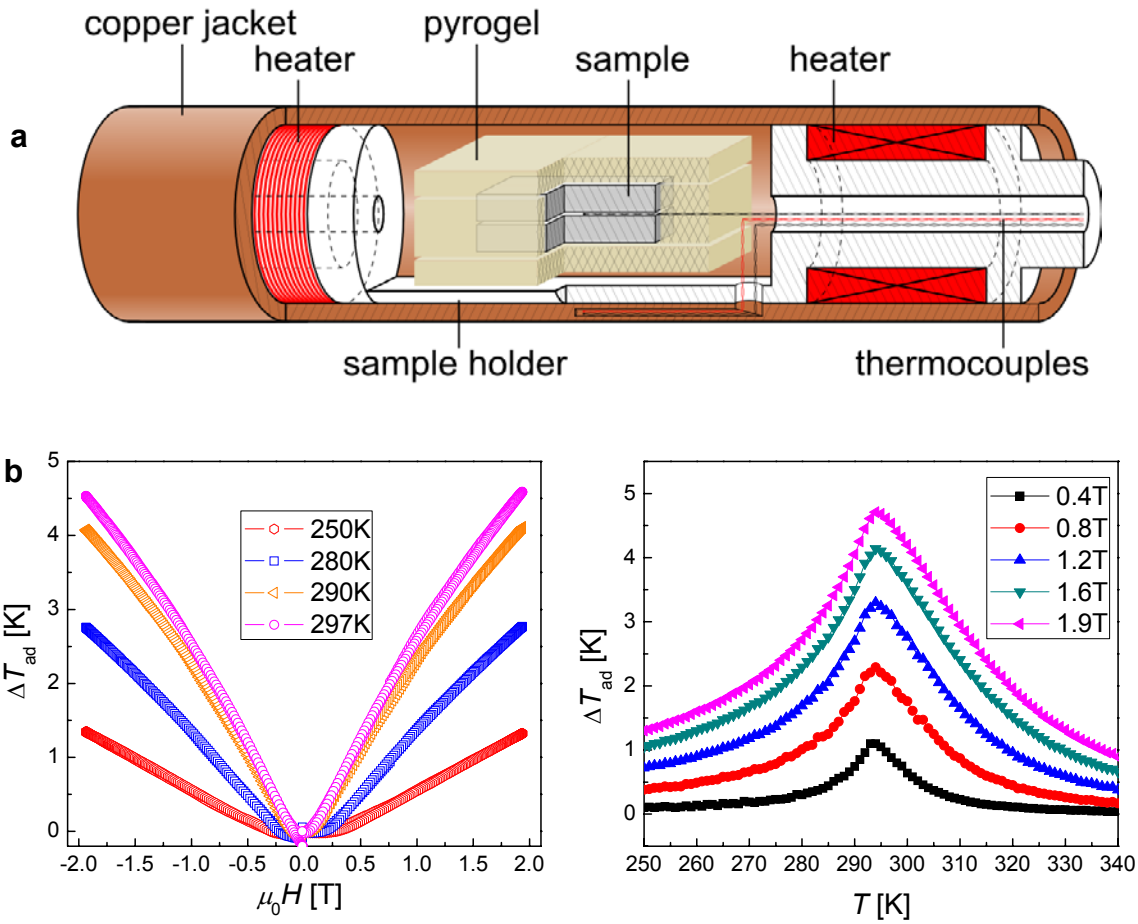

Supplementary Figure S4:
Schematic of adiabatic temperature change measurement cell (**a**) and field and temperature dependence of adiabatic temperature change of a polycrystalline Gd sample (**b**).